JOURNAL OF MATERIALS SCIENCE: MATERIALS IN MEDICINE **16** (2005) 1137– 1142

Novel deposition of nano-sized silicon substituted hydroxyapatite by electrostatic spraying

J. HUANG[1], S. N. JAYASINGHE[2], S. M. BEST[1], M. J. EDIRISINGHE[2], R. A. BROOKS[3], N. RUSHTON[3], W. BONFIELD[1]
[1]*Department of Materials Science and Metallurgy, University of Cambridge, Pembroke Street, Cambridge CB2 3QZ, UK*
[2]*Department of Materials, Queen Mary, University of London, Mile End Road, London E1 4NS, UK*
[3]*Orthopaedic Research Unit, Box 180, Addenbrooke's Hospital, Hills Road, Cambridge CB2 2QQ, UK*

Suspensions containing nano-sized silicon substituted hydroxyaptite (nSiHA) particles were produced and processed for electrostatic spray deposition. No secondary phases were detected by X-ray diffraction, which indicated that the nSiHA was phase pure. Electrostatic spraying of nSiHA in cone-jet mode was achieved at flow rate of 10^{-9} m^3s^{-1} with an applied voltage between the needle and the ring-shaped ground electrode set at 6 to 8 kV. Micrometer- and submicrometer-scaled islands of nSiHA have been deposited on glass and titanium substrates. The surface roughness of such nHA and nSiHA islands was in the range 60 to 80 nm, as measured from atomic force microscopy in tapping mode. The growth of primary human osteoblast (HOB) cells on the nSiHA deposited substrates increased with time during the 4 days of culture, and the increase was related with the Si content in substituted HA, indicating that nSiHA was able to promote and support the growth of HOB cells. Scanning electron microscopy (SEM) revealed that extracellular matrix (ECM) produced by the HOB cells on these nSiHA deposits was well organized. In addition, the presence of Ca and P containing nodules in the ECM were also confirmed by Energy Dispersive X-ray (EDX) analysis, indicating early signs of calcification fronts. The results showed that nSiHA produced by electrostatic spray deposition was able to promote the attachment and the growth of HOB cells. Therefore, electrostatic spray deposition offers great potential for the creation of bioactive surfaces to provide improved interfacial bonding with host tissues.

1. Introduction

Metallic implants have been widely used in major load-bearing applications, such as hip prostheses and dental implants due to their high strength. However, there is no direct bone bonding to most metals. The most successful approach to solve this problem to date has been the use of bioactive hydroxyapatite (HA) coatings [1]. It has recently been discovered that the *in vitro* and *in vivo* bioactivity of HA can be significantly improved with the incorporation of silicate ions into the HA structure [2–6], making silicon substituted hydroxyapatite (Si-HA) an attractive alternative to conventional HA in bone replacement. Various low temperature thin film techniques have been developed to extend the clinical application of HA coated implants where conventional thermal plasma spraying has been unable to deliver the required outcome. These techniques include magnetron sputtering, biomimetic coating and, more recently, electrostatic spray deposition, also called electrospraying, electrostatic atomisation or electrohydrodynamic atomisation [7–14].

Electrostatic spray deposition has the great advantage of creating a controlled and defined surface topography, a feature that is known to affect biological response. Therefore, in order to achieve more rapid bone apposition against the implant, our approach is to deposit the highly bioactive Si-HA onto implant surfaces with a surface topography to further enhance the biological response. In this study, electrostatic spray deposition of nano-sized Si-HA has been performed and this represents a new way to modify the implant surface to achieve the goal of improving bone integration.

2. Materials and methods

2.1. Preparation of nHA and nSiHA

Nano-scaled Si-HA crystallites containing 0, 0.8, 1.2 and 1.6 wt% of Si were synthesised based on the

TABLE I Molar concentration of reagents used for making nSiHA

Reagent	0 wt% SiHA	0.8 wt% SiHA	1.2 wt% SiHA	1.6 wt% SiHA
$Ca(OH)_2$	0.5	0.5	0.5	0.5
H_3PO_4	0.3	0.286	0.279	0.272
TEOS	0	0.014	0.021	0.028
Ca/P	1.67	1.75	1.79	1.84
Ca/(P + Si)	1.67	1.67	1.67	1.67

reaction between calcium hydroxide ($Ca(OH)_2$) and orthophosphoric acid (H_3PO_4) (AnalaR grade, BDH, UK). Tetraethoxysilane (TEOS) was used for the source of Si, while Ca/(Si+P) ratios were maintained at 1.67, as detailed in Table I. P and Si solutions were added drop-wise to the Ca solution under continuous stirring at room temperature, while the pH was kept above 10.5 by the addition of ammonia solution. The stirring was maintained for a further 16 h after complete addition of the reactants. The precipitate obtained was washed thoroughly with boiling deionised water and further aged. Ethanol (AnalaR grade, Fisher Scientific, UK) was used to disperse the particles for preparation of nHA and nSiHA suspensions.

2.2. Characterisation of suspensions

The morphology of nSiHA was examined using a JEOL 200CX transmission electron microscope. Phase composition analysis was carried out on a Philips PW1730 X-ray diffractometer using CuK_α radiation, operated at 40 kV and 40 mA. Data were collected from 20 to 40 ° with a step size of 0.05 ° and a scan time of 6 s was used.

The viscosity of the nSiHA suspensions was measured using ViscoEasy and AVS360 viscometers (Camlab Ltd, Cambridge, UK). The DC conductivity of nSiHA suspensions was determined using a Hanna HI 8733 conductivity probe (Camlab Ltd, Cambridge, UK). The suspensions were subjected to loss-on-ignition experiments to determine the concentration of nSiHA particles.

2.3. Electrostatic spraying of nSiHA suspensions

Electrostatic spraying was carried out using the equipment shown in Fig. 1A stainless steel needle with an inner diameter of ~500 μm and a ring-shaped ground electrode were used to produce the spray. Freshly prepared suspension was syringed to the needle at the flow rate of 10^{-9} m^3s^{-1} with the applied voltage between the needle and the ring-shaped ground electrode set at 6 to 8 kV and subsequently electrostatic spraying was attempted. Titanium and glass substrates were placed underneath the ground electrode to be deposited with nSiHA.

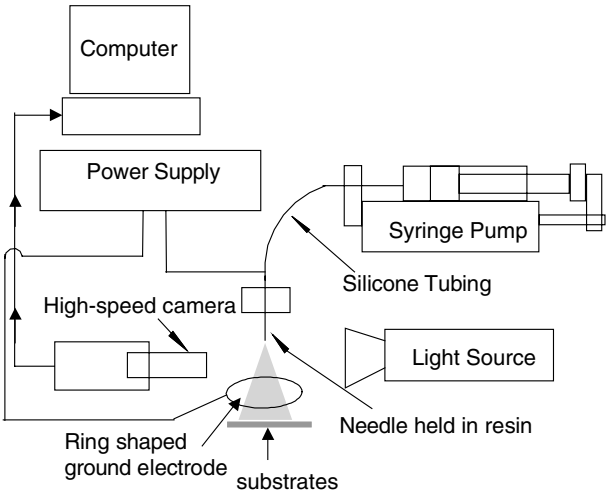

Figure 1 Schematic diagram of the electrostatic spraying set-up for nSiHA deposition.

2.4. Characterisation of nSiHA deposition

The structure of nSiHA relics on glass and titanium substrates was examined using a JEOL 6340 field emission SEM at an accelerating voltage of 5 keV after coating with a thin layer of platinum. The surface roughness of nSiHA relics on the glass substrate was measured by atomic force microscopy (Digital instrument, nanoscope III). The equipment was operated in tapping mode, topographic images were constructed by scanning the tip above the surface.

2.5. *In vitro* study

A primary human osteoblast (HOB) cell (Promocell, GmbH) model was used to assess the biological response of nSiHA deposited surface. The glass substrates (10 × 10 mm) with nHA and nSiHA deposits were sterilised by dry heat at 600 °C for 4 h. HOB cells (2×10^4 cells) were then seeded directly on the surface of these substrates and incubated at 37 °C in a humidified air atmosphere of 5% CO_2. The growth of HOB cells on the nHA and nSiHA deposits was monitored regularly by examination using optical microscopy and was determined after the intervals of 2 and 4 days of culturing by alamarBlue™ assay (Serotec, Oxford, UK), which measured the metabolic activity of cells. The

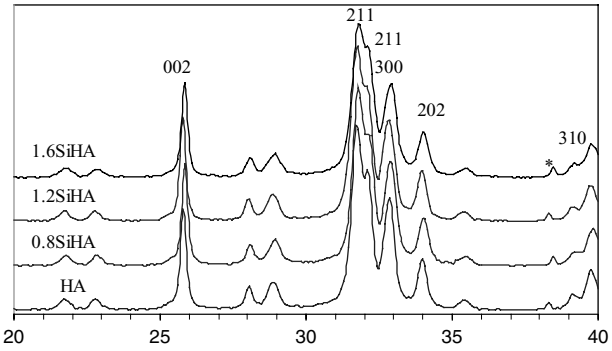

Figure 2 X-ray diffraction patterns of nHA, 0.8, 1.2 wt% nSiHA and 1.6 wt% nSiHA, Al (100) peak observed at 38.5 ° 2θ was from aluminum holder used.

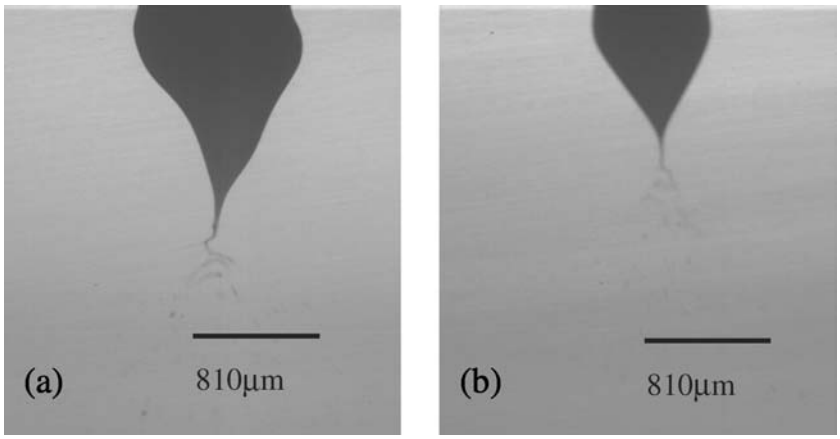

Figure 3 Electrospraying of the (a) nHA and (b) 0.8 wt% nSiHA suspension in cone-jet mode as captured by a Phantom *V* 7 high-speed camera (Photo-Sonics International Ltd, Oxford, UK).

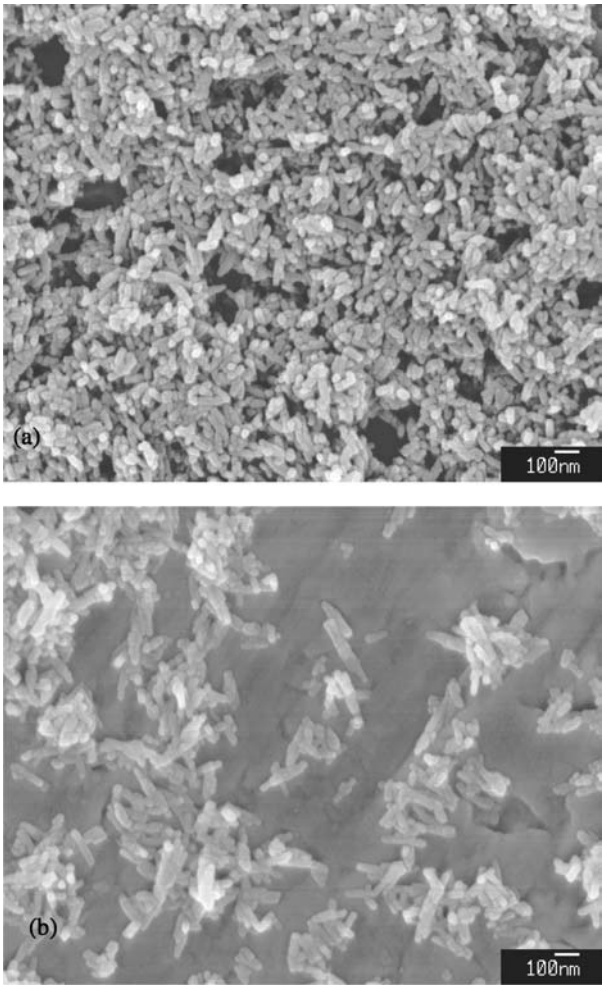

Figure 4 SEM micrograph of deposits of (a) nHA and (b) 1.6 wt% nSiHA on titanium substrates.

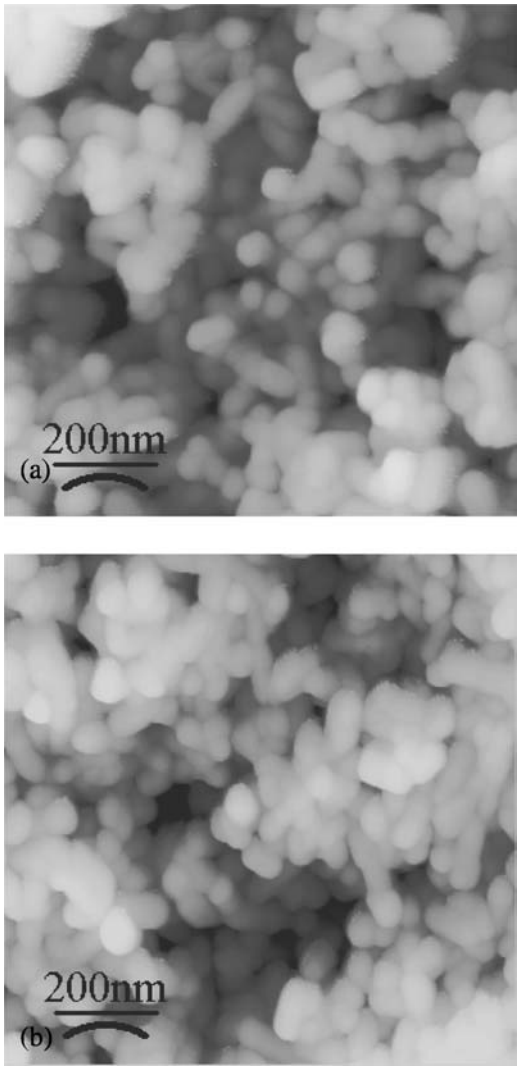

Figure 5 AFM image of (a) nHA and (b) 0.8 wt% nSiHA relics after heat treatment at 600 °C for 4 h.

absorbance at wavelength of 570 nm was measured on a plate reader with a reference wavelength of 600 nm. A calibration study with a range of cell density was performed, and the absorbance obtained was proportional to cell numbers. A *t*-test was used to determine whether any significant differences existed between the mean values of absorbance measured. A difference was considered to be significant at $p < 0.05$.

2.6. Immunofluorescence and cytoskeletal observation

After 24 h in culture, the cells on the substrates were fixed in 4% paraformaldehyde/PBS with 1% sucrose for 15 min, the samples were then washed with PBS, permeabilised at 4 °C for 5 min. The samples were incubated with 1% bovine serum albumin (BSA)/PBS

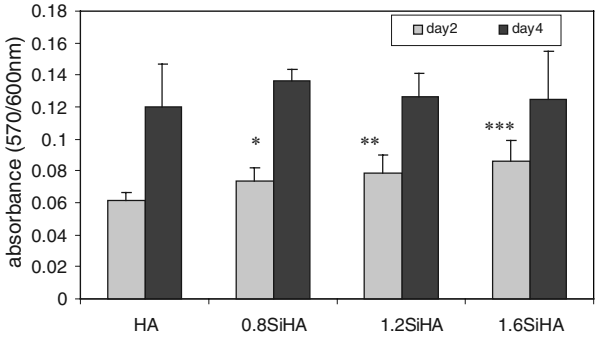

Figure 6 Comparison of the absorbance of primary human osteoblast (HOB) cells on nHA and nSiHA deposits during 4 days of culture by alamarBlue assay, the cell numbers on 0.8, 1.2 and 1.6 wt.% SiHA was significantly higher than that on nHA at day 2 ($^{*}p = 0.0012$, $^{**}p = 0.006$ and $^{***}p < 0.0001$, respectively).

at 37 °C for 5 min to block the non-specific binding. This step was followed by the addition of TRITC conjugated phalloidin (Sigma, Poole, UK) at 37 °C for 1 h. The samples were then mounted in a Vectorshield fluorescent mountant (Vector Laboratories, UK), then viewed by a Leica SP2 laser scanning confocal microscope.

2.7. Attachment of HOB cells on nSiHA deposits

The ability of nSiHA to promote the formation of focal contacts of cells was studied by SEM. After 3 days culturing of HOB cells on the nSiHA deposits, the cultures were fixed, stained with 1% osmium tetroxide and dehydrated in a graduated series of alcohols and finally critical point dried (Polaron E3000 CPD). The sample surface was coated with a thin layer of palladium before it was examined using a JEOL 6340 field emission SEM.

TABLE II Electrostatic spray deposition parameters of nHA and nSiHA suspensions and their viscosities and DC electrical conductivities

	0 wt% SiHA	0.8 wt% SiHA	1.2 wt% SiHA	1.6 wt% SiHA
Filler content (wt%)	4.3	5.8	8.8	5.3
Applied voltage (kV)	6.2	8.4	8.4	7.8
Flow rate ($m^3\ s^{-1}$)	10^{-9}	10^{-9}	10^{-9}	10^{-9}
Viscosity (mPa s)	321	425	487	400
DC electrical conductivity (Sm^{-1})	5.59×10^{-4}	5.09×10^{-4}	4.83×10^{-4}	5.95×10^{-4}

3. Results and discussion

3.1. nSiHA suspensions

The morphology of both the nHA and the nSiHA particles was similar, and particles were rod–like with dimension of 20–30 nm in width and 50–80 nm in length. X-ray diffraction (XRD) patterns of nSiHA revealed the presence of all the major HA peaks, (002), (211), (300), (202) and (310), as shown in Fig. 2. No secondary phases, such as tricalcium phosphate and calcium oxide, were detected, which confirmed the phase purity of the nSiHA produced.

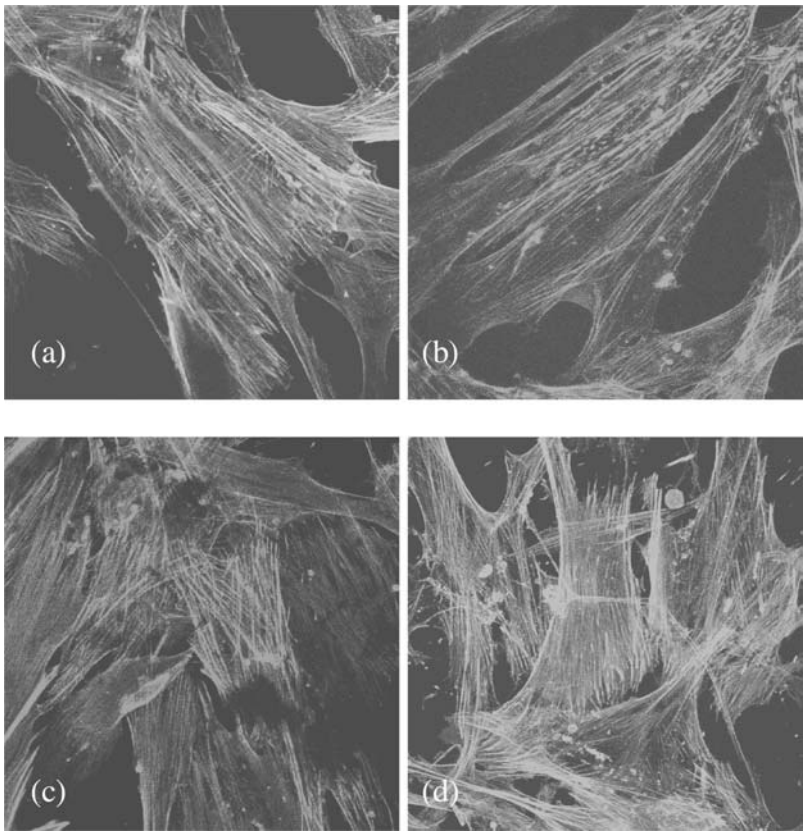

Figure 7 The cytoskeletal organisation of HOB cells on (a) nHA, (b) 0.8 wt%, (c) 1.2 wt% and (d) 1.6 wt% nSiHA deposited substrate after 24 h in culture, HOB cells were flattened with normal stress fibres actin organization.

The viscosity and dc conductivity of the nHA and nSiHA suspensions were compared, as shown in Table II. The viscosity of the nSiHA suspension was higher than that of the nHA suspension. However, the viscosities measured were lower compared with alumina ceramic suspensions [15]. Therefore, there is more scope to concentrate the suspension if necessary. The DC conductivity of nSiHA and nHA suspensions was similar reflecting the low filler contents.

3.2. Electrostatic spraying

A cone-jet mode of electrostatic atomisation was achieved using the nHA and nSiHA suspensions, as shown in Fig. 3. Electrostatic spray deposition was then carried out to deposit fine relics on the substrates. Micrometer- to submicrometer-scaled nSiHA islands were successfully deposited on the substrate surface, as shown in Fig. 4. Rod-like particles of nHA and nSiHA about 50 to 80 nm in length were observed, they clustered together to form islands. The surface topography of nHA and nSiHA were viewed by atomic force microscopy (Fig. 5), which also revealed that the mean surface roughness of the deposit of nHA and nSiHA was 80 and 60 nm, respectively.

3.3. alamarBlue™ assay

The growth of HOB cells on the nSiHA deposited substrates increased with Si content in substituted HA during the *in vitro* culture (Fig. 6). The numbers of HOB cells on 0.8, 1.2 and 1.6 wt% nSiHA was significantly higher than that on nHA at day 2, indicating that nSiHA was able to promote cell attachment. The results also showed that the HOB cells increased with culture time during 4 days of culture on nHA and nSiHA deposits, therefore, these deposits were able to support the growth of HOB cells.

3.4. Cytoskeletal observation

The development of the cell cytoskeleton on nSiHA deposits was studied by immuno-fluorescent staining of actin cytoskeletal proteins to understand the quality of cell adhesion. Immunofluorescent staining at 24 h of culture revealed initial interactions between HOB cells and the nSiHA. Cells could be seen to have actin stress fibres throughout their cytoskeletons on the nSiHA deposited substrate (Fig. 7).

3.5. The attachment and growth of HOB cells

HOB cells were able to attach to the nHA sprayed substrates (Figs. 8(a)–(d)) and maintained their osteoblastic morphology with filapodia preferably attached to nHA particles (Fig. 8(c)). There were large areas of confluent cells after 3 days of culture and fibre-like extracellular matrices (ECM) were produced (Fig. 8(b)). There were larger amounts of ECM produced by the HOB cells on nSiHA deposits. They were well organized, and plenty of spherical nodules were observed attached and/or embedded in the ECM (Fig. 8(d)). Energy dispersive X-ray (EDX) analysis revealed that these nano-sized nodules contained Ca and P, which indicate the early stages of bone mineralisation.

The results obtained from this study support the previous findings that the presence of Si in SiHA was able to stimulate the HOB cell activity *in vitro* [2], which might be able to enhance bone formation *in vivo*. It is well recognised that Si plays a critical role in the bone calcification process [16]. Reffitt *et al.* found out that soluble silicon was able to stimulate collagen Type 1 synthesis in human osteoblast-like cells and enhances osteoblastic differentiation [17]. Porter *et al.* showed that incorporation of Si into HA structure accelerated the dissolution process *in vivo*, which in turn contributed to the enhanced bioactivity of SiHA [5].

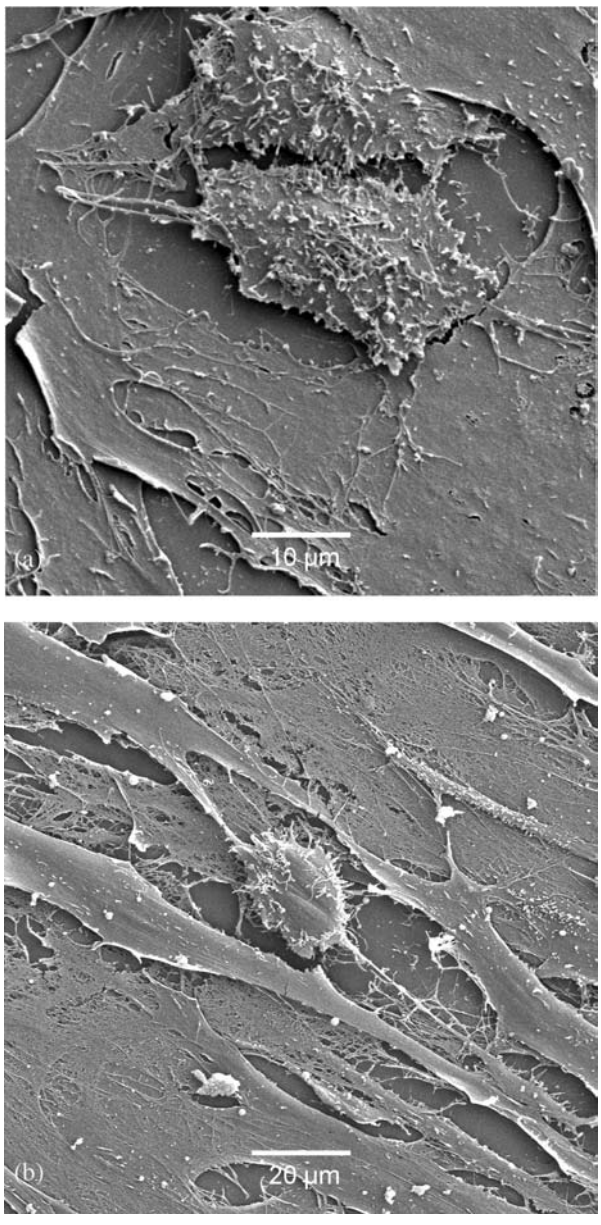

Figure 8 Morphology of HOB cells on the surface of nHA (a and c) and 1.6 wt% nSiHA (b and d) after 3 days culturing. HOB cells maintained osteoblast morphology with filapodia attached to nanosized HA (c) and well organized extracellular matrix produced by HOB cells (d), spherical nodules were rich in Ca and P from EDX analysis. (*Continued*.)

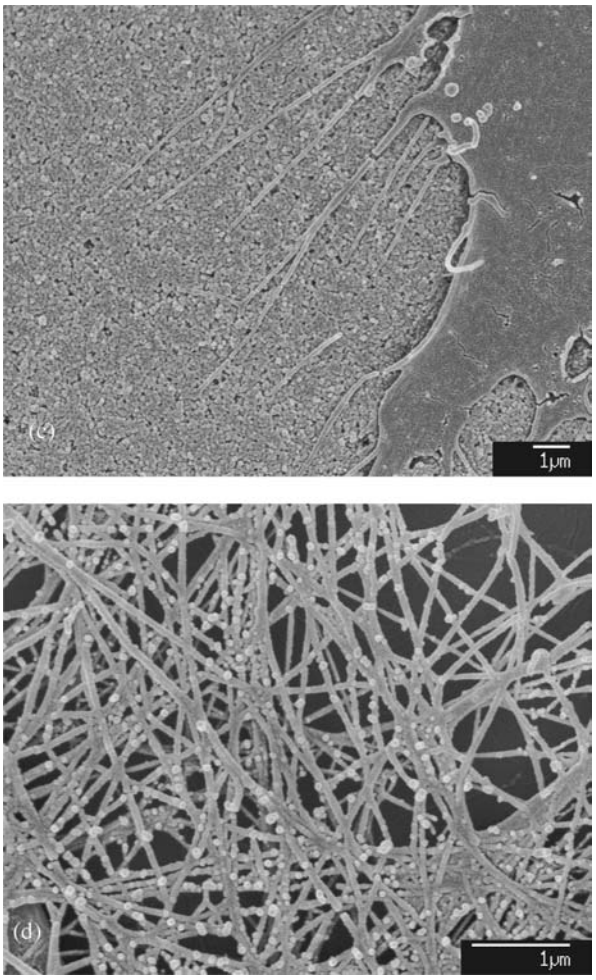

Figure 8 (*Continued*).

From this preliminary study, the stimulatory effect on human osteoblast cell activity of nano-sized silicon substituted hydroxyapatite deposited by electrospraying is very encouraging. It indicates that combining materials chemistry with surface topography could play a very important role in future design of medical implants.

4. Conclusions

Bioactive SiHA deposition has been achieved by electrostatic spraying of nano-sized SiHA suspension. This provided a favourable surface for attachment and growth of HOB cells. Therefore, electrostatic spray deposition offers great potential for the creation of bioactive surfaces and hence providing improved interfacial bonding with host tissues.

Acknowledgments

The financial support of UK EPSRC (Grants GR/S71996, GR/S97880 & GR/S97873) is gratefully acknowledged.

References

1. L. PALM, S. JACOBSSON and I. IVARSSON, *J. Arthrop.* **17** (2002) 172.
2. I. R. GIBSON, J. HUANG, S. M. BEST and W. BONFIELD, in "Bioceramics" edited by H. Ohgushi, G. W. Hastings and T. Yoshikawa (World Scientific, Singapore 1999) vol 12, p. 191.
3. N. PATEL, S. M. BEST, W. BONFIELD, I. R. GIBSON, K. A. HING, E. DAMIEN and P. A. REVELL, *J. Mater. Sci Mater Med.* **13** (2002) 1199.
4. F. BALAS, J. PEREZ-PARIENTE and M. VALLET-REGI, *J. Biomed. Mater Res.* **66A** (2003) 364.
5. A. E. PORTER, N. PATEL, J. N. SKEPPER, S. M. BEST and W. BONFIELD, *Biomaterials* **24** (2003) 4609.
6. *idem.*, *ibid.* **25** (2004) 3303.
7. J. HUANG, S. N. JAYASINGHE, S. M. BEST, M. J. EDIRISINGHE, R. A. BROOKS and W. BONFIELD, *J. Mater. Sci.* **39** (2004) 1029.
8. J. E. G. HULSHOFF, K. VAN DIJK, J. P. C. M. VAN DER WAERDEN, J. G. C. WOLKE, W. KALK and J. A. JANSEN, *J. Biomed. Mater. Res.* **31** (1996) 329.
9. E. S. THIAN, J. HUANG, S. M. BEST, Z. H. BARBER and W. BONFIELD, *Biomaterials* **26** (2005) 2947.
10. *idem.*, *J. Mater. Sci. Mater. Med.* **16** (2005) 411.
11. W. Q, YAN, T. NAKAMURA, K. KAWANABE, S. NISHIGOCHI, M. OKA and T. KOKUBO, *Biomaterials* **18** (1997) 1185.
12. Y. LIU, K. DE GROOT and E. B. HUNZIKER, *Bone* **36** (2005) 745.
13. S. C. G. LEEUWENBURGH, J. G. C. WOLKE, J. SCHOONMAN and J. A. JANSEN, *Thin Solid Films* **472** (2005) 105.
14. M. C. SIEBERS, X. F. WALBOOMERS, S. C. G. LEEUWENBURGH, J. G. C. WOLKE and J. A. JANSEN, *Biomaterials* **25** (2004) 2019.
15. S. N. JAYASINGHE and M. J. EDIRISINGHE, *J. Euro. Ceram. Soc.* **24** (2004) 2203.
16. E. M. CARLISLE, *Science* **167** (1970) 279.
17. D. M. REFFITT, N. OGSTON, R. JUGDAOHSINGH, H. F. J. CHEUNG, B. A. J. EVANS, R. P. H. THOMPSON, J. J. POWELL and G. N. HAMPSON, *Bone* **32** (2003) 127.

Received 29 June
and accepted 19 August 2005